A Major Quantitative Trait Locus for Cadmium Tolerance in *Arabidopsis halleri* Colocalizes with *HMA4*, a Gene Encoding a Heavy Metal ATPase[1][OA]

Mikael Courbot[2,3], Glenda Willems[2], Patrick Motte, Samuel Arvidsson, Nancy Roosens, Pierre Saumitou-Laprade, and Nathalie Verbruggen*

Laboratoire de Physiologie et de Génétique moléculaire des Plantes, Université Libre de Bruxelles, B–1050 Brussels, Belgium (M.C., G.W., S.A., N.V.); Laboratoire de Génétique et Evolution des Populations Végétales, Unité Mixte de Recherche Centre National de la Recherche Scientifique 8016, FR Centre National de la Recherche Scientifique 1818, Université de Lille 1, F–59655 Villeneuve d'Ascq cedex, France (G.W., N.R., P.S.-L.); and Laboratory of Plant Cell and Molecular Biology and Center for Assistance in Technology of Microscopy, University of Liège, B–4000 Liege, Belgium (P.M.)

Cadmium (Cd) tolerance seems to be a constitutive species-level trait in *Arabidopsis halleri* sp. *halleri*. Therefore, an interspecific cross was made between *A. halleri* and its closest nontolerant interfertile relative, *Arabidopsis lyrata* sp. *petraea*, and a first-generation backcross population (BC1) was used to map quantitative trait loci (QTL) for Cd tolerance. Three QTL were identified, which explained 43%, 24%, and 16% of the phenotypic variation in the mapping population. *Heavy metal transporting ATPases4* (*HMA4*), encoding a predicted heavy metal ATPase, colocalized with the peak of the major QTL Cdtol-1 and was consequently further studied. *HMA4* transcripts levels were higher in the roots and the shoots of *A. halleri* than in *A. lyrata* sp. *petraea*. Furthermore, *HMA4* was also more highly expressed in all BC1 genotypes harboring the *HMA4 A. halleri* allele at the QTL Cdtol-1, independently of the presence of an *A. halleri* allele at the two other QTL. Overexpression of *AhHMA4* in yeast (*Saccharomyces cerevisiae*) supported a role of HMA4 in zinc (Zn) and Cd transport by reducing the Cd and Zn contents of the yeast cells. In epidermal tobacco (*Nicotiana tabacum*) cells, AhHMA4:green fluorescent protein was clearly localized in the plasma membrane. Taken together, all available data point to the elevated expression of HMA4 P_{1B}-type ATPase as an efficient mechanism for improving Cd/Zn tolerance in plants under conditions of Cd/Zn excess by maintaining low cellular Cd^{2+} and Zn^{2+} concentrations in the cytoplasm.

Pollutants such as heavy metals can occur at very high concentrations in the soil as a consequence of either ancient natural processes or recent human activities such as mining, industrial, and agricultural practices. Although heavy metals are very toxic at high concentrations, some metal-tolerant plant species have developed the ability to grow and reproduce on soils highly polluted by heavy metals (Macnair, 1987). Among those metal-tolerant plants, some possess a remarkable physiological trait called hyperaccumulation that enables them to tolerate and accumulate high heavy metal concentrations in their shoots (about 100 times those occurring in nonaccumulator plants growing in the same substrates). Metal hyperaccumulators are consequently a particularly valuable resource to study the genetic basis of metal homeostasis.

Arabidopsis halleri is an emerging model species for the molecular elucidation of metal tolerance and hyperaccumulation (Becher et al., 2004; Weber et al., 2004; Craciun et al., 2006; Filatov et al., 2006). This species belongs to the family Brassicaceae and shares about 94% DNA sequence identity within coding regions with the non-metal-tolerant plant species Arabidopsis (*Arabidopsis thaliana*; Becher et al., 2004). *A. halleri* constitutively tolerates zinc (Zn; Pauwels et al., 2006) and so far all the identified accessions are able to tolerate cadmium (Cd) and to hyperaccumulate Zn (Macnair et al., 1999). Hyperaccumulation of Cd was

[1] This work was supported by the European Union (Research Training Network METALHOME, grant no. HPRN–CT–2002–00243), the Belgian Science Policy (Interuniversity Attraction Pole Programme V/13 and VI/33), and the Fonds National de la Recherche Scientifique (grant no. Fonds de la Recherche Fondamentale Collective 2.4565.02) at the Université Libre de Bruxelles. At the Université de Lille (Unité Mixte de Recherche Centre National de la Recherche Scientifique 8016), research was supported by the European Union (Research Training Network, *METALHOME*, grant no. HPRN–CT–2002–00243), Contrat de Plan Etat/Région Nord-Pas de Calais, the European Fonds Européens de Développement Régional (contract no. 79/1769), the Programme National Action Concentrée Incitative-Fonds National de la Science "Ecosphère Continentale" (contract no. 04 2 9 FNS), and a Marie Curie Intra-European Fellowship (proposal no. 024683 METOLEVOL).

[2] These authors contributed equally to the article.

[3] Present address: Department of Plant Sciences, University of Oxford, Oxford OX1 3RB, UK.

* Corresponding author; e-mail nverbru@ulb.ac.be; fax 32–2–650–54–21.

The author responsible for distribution of materials integral to the findings presented in this article in accordance with the policy described in the Instructions for Authors (www.plantphysiol.org) is: Nathalie Verbruggen (nverbru@ulb.ac.be).

[OA] Open Access articles can be viewed online without a subscription.
www.plantphysiol.org/cgi/doi/10.1104/pp.106.095133

observed in at least one *A. halleri* population (Auby, France; Bert et al., 2002, 2003).

Metal tolerance and hyperaccumulation are thought to have evolved through adaptations of metal homeostasis processes including metal uptake, chelation, trafficking, and storage (Pence et al., 2000; Pollard et al., 2002; Krämer, 2005; Clemens, 2006). To identify the genes governing these traits, numerous studies have been performed. For instance, segregation analyses of crosses between nontolerant and tolerant individuals indicated that a single gene or a small number of genes govern metal tolerance (Schat and Ten Bookum, 1992; Macnair et al., 1999). More recently, molecular and functional studies were performed on various metal homeostasis genes to determine their role in metal tolerance and/or hyperaccumulation. Also, microarray and cDNA-amplified fragment length polymorphism analyses were applied to hyperaccumulator species to identify genes differentially regulated under various metal conditions in nontolerant nonhyperaccumulator versus tolerant hyperaccumulator species (Craciun et al., 2006; van de Mortel et al., 2006). Very recently, quantitative trait loci (QTL) mapping was used to identify the chromosomal regions involved in Zn and Cd hyperaccumulation in the hyperaccumulator species *Thlaspi caerulescens*. Two QTL were identified for Zn and Cd accumulation in roots, while three QTL and one QTL were reported for Zn and Cd accumulation, respectively, in shoots (Deniau et al., 2006). But, in contrast to *Thlaspi* there is a possibility of identifying individual genes in *A. halleri* because of its close relationship to Arabidopsis.

In this work, QTL mapping was performed to identify the genes underlying Cd tolerance in *A. halleri*. Because no Cd-sensitive accession has been identified so far in *A. halleri*, a first-generation backcross progeny of *A. halleri* sp. *halleri* (pollen donor) and its nontolerant relative *Arabidopsis lyrata* sp. *petraea* (pollen recipient) was produced (Bert et al., 2003) and used for the QTL analysis of Cd tolerance. The *A. halleri* genotype used in this study originated from a metallicolous population, previously shown to be tolerant to high Zn and Cd concentrations and able to hyperaccumulate those metals. The gene *heavy metal transporting ATPases4* (*HMA4*) was found to colocalize with the major QTL and was consequently focused on in this study.

The P_{1B}-type ATPases, also known as the HMAs, play an important role in transporting transition metal ions against their electrochemical gradient using the energy provided by ATP hydrolysis. They have been identified in all living organisms from archaea to humans, including yeast (*Saccharomyces cerevisiae*) and plants. The HMAs cluster into two classes: those transporting monovalent cations (copper [Cu]/silver [Ag] group) and those transporting divalent cations (Zn/cobalt [Co]/Cd/lead [Pb] group; Axelsen and Palmgren, 2001). Although all classes of P_{1B}-type ATPases have been detected in prokaryotes (Rensing et al., 1999), in nonplant eukaryotes only Cu/Ag P_{1B}-type ATPases have been identified to date. Arabidopsis and *Oryza sativa* contain eight *HMA* genes (Baxter et al., 2003), suggesting that these enzymes play important roles in the transport of metals in plants. In Arabidopsis, analysis of the complete genome sequence predicts the distribution of these eight HMAs in two classes: HMA1-4 for the transport of Zn/Co/Cd/Pb and HMA5-8 for Cu/Ag.

HMA4 was the first plant P_{1B}-type ATPase of the divalent transport group to be cloned and characterized in Arabidopsis (Mills et al., 2003). A role for HMA4 in Zn homeostasis and Cd detoxification, and in the translocation of these metals from the root to the shoot, has been demonstrated in Arabidopsis (Mills et al., 2003, 2005; Hussain et al., 2004; Verret et al., 2004, 2005).

In this study, HMA4 was cloned and functionally characterized in *A. halleri*.

RESULTS

QTL Mapping of Cd Tolerance

The QTL for Cd tolerance were identified on the *A. halleri* × *A. lyrata* sp. *petraea* genetic linkage map (henceforth called the *Ah* × *Alp* map), which was constructed on 196 individuals of the *A. halleri* × *A. lyrata* sp. *petraea* backcross population (BC1) progeny (henceforth called BC1 progeny; Willems et al., 2007). On this linkage map, a total of 85 markers was distributed on eight linkage groups (LGs), corresponding to the haploid chromosome number of both parental genotypes. Significant segregation at a locus-by-locus significance level of 0.05 was found for 40% of the markers. All markers showed an excess of the homospecific *A. lyrata* sp. *petraea* 1/*A. lyrata* sp. *petraea* 2 genotypes compared to the heterospecific *A. halleri*/*A. lyrata* sp. *petraea* 2 genotypes. Because we applied stringent goodness-of-fit thresholds to minimize the effects of segregation distortion and observed a high degree of macrosynteny with the Arabidopsis genome and the recently published linkage map of *A. lyrata* sp. *petraea* (Kuittinen et al., 2004), the *Ah* × *Alp* map is assumed to be robust.

A highly significant genotype effect of Cd tolerance ($P < 0.0001$) was revealed through an ANOVA analysis, performed on the 100% effective concentration (EC100), i.e. the lowest concentration at which no new root growth was observed, values obtained on 79 BC1 individuals. A high broad-sense heritability of 0.89 was obtained for this trait in the mapping population.

We performed the QTL analysis of Cd tolerance on the $EC100_{max}$ values, corresponding to the maximum tolerance level of the BC1 genotypes characterized for Cd tolerance. Three QTL for Cd tolerance, showing a log of the odds (LOD) score exceeding the significance threshold of 2.4 ($\alpha = 0.05$), were detected on the LGs LG3, LG4, and LG6 of the *Ah* × *Alp* linkage map (Fig. 1) through Multiple QTL Mapping (MQM; MapQTL 4.0; Van Ooijen et al., 2002). Their significance was

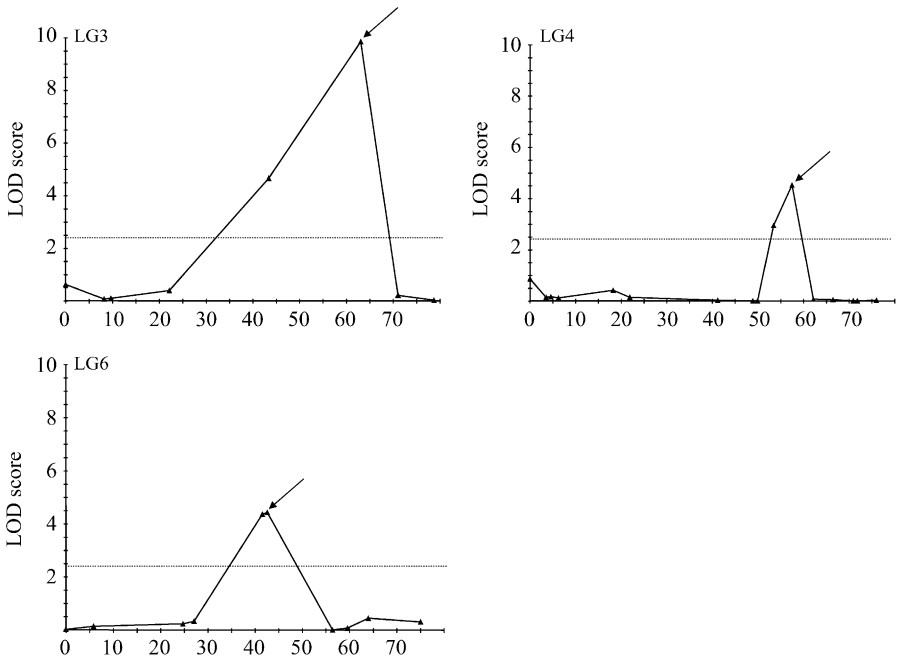

Figure 1. QTL for Cd tolerance in the *Ah* × *Alp* BC1 progeny. LOD score profiles are given along the LGs LG3, LG4, and LG6, on which the QTL for Cd tolerance were identified. Map positions are plotted along the abscissa. LOD scores are plotted along the *y* axis. Dashed lines correspond to the LOD score threshold (2.4) for QTL detection at an error level $\alpha = 0.05$. QTL are indicated by arrows above the LOD score profile.

verified through a nonparametric Kruskal-Wallis test ($P < 0.0001$, $P < 0.0001$, $P < 0.005$). The QTL Cdtol-1, Cdtol-2, and Cdtol-3 explained 42.9%, 23.7%, and 15.9% of the phenotypic variance, respectively (Table I). Together they accounted for 82.5% of the phenotypic variance, or for 92.7% of the genetic variance observed for Cd tolerance in the BC1 progeny. At all three QTL, the *A. halleri* allele had a positive effect on Cd tolerance. The increase in Cd tolerance due to the presence of the *A. halleri* allele, however, was greater for the QTL Cdtol-1 than for the other QTL (Table I). BC1 individuals harboring the *A. halleri* allele at QTL Cdtol-1 showed a nearly 2-fold increase in Cd tolerance when compared to BC1 genotypes carrying the *A. lyrata* sp. *petraea* allele, independently of the presence of the *A. halleri* allele at the two other QTL (Fig. 2). One significant epistatic interaction was revealed between the QTL Cdtol-1 and Cdtol-3 at a low significance threshold ($P = 0.022$; Table II). However, using log-transformed Cd tolerance data, the significance of the epistatic interaction between the QTL Cdtol-1 and Cdtol-3 was lost ($P = 0.294$), indicating most probably a statistical artifact (Table II). The QTL for Cd tolerance are consequently inferred to be mainly additive.

Marker Densification in the Major QTL Region

The *HMA4* locus was located at the maximum LOD score position of the major QTL for Cd tolerance, Cdtol-1, explaining up to 48.2% of the genetic variance observed for this trait in the *Ah* × *Alp* BC1 progeny (Fig. 3A). To narrow down the confidence interval associated with this QTL and, assuming a high degree of synteny between Arabidopsis and *A. halleri*, the genes *At2g10940*, *At2g14620*, and *At2g18196* were selected based on their position in the Arabidopsis genome. As expected, these markers mapped to LG3 of the *Ah* × *Alp* map in the same order as in Arabidopsis. The mapping of these markers increased the accuracy of the QTL Cdtol-1 and reinforced its colocalization with the *HMA4* locus (Fig. 3B).

AhHMA4 Cloning and Sequence Analysis

Because of the importance of HMA4 in the Cd tolerance of *A. halleri*, we decided to investigate the possible specificities of *Ah*HMA4. To isolate a full-length cDNA for *AhHMA4*, a reverse transcription (RT)-PCR approach was taken. The 3,486-bp *AhHMA4* cDNA was directly cloned into pYES2-GFP plasmid. According to its nucleotide sequence, AhHMA4 belongs to the P_{1B}-type ATPases involved in metal transport.

The deduced 1,161 amino acid sequence of AhHMA4 was aligned with the Arabidopsis sequence of HMA4 (AtHMA4) and with the *T. caerulescens* sequence of HMA4 (TcHMA4; Fig. 4), with which it shares 80% and 70% identity, respectively. Whereas the sequence of the N-terminal part (AhHMA4-N, amino acid position 1–720, between the start codon and the end of the last transmembrane span) was highly similar in the three HMA4 sequences (95% identity with AtHMA4 and 89% with TcHMA4), the sequence of the C-terminal part (AhHMA4-C, amino acid position 720–1,161, between the end of the last transmembrane span and the stop codon) was more divergent (59% identity with AtHMA4 and 46% with TcHMA4). No specific features were observed for AhHMA4 compared to At- or TcHMA4 homologs.

Table I. *QTL for Cd tolerance*

QTL[a]	LG Marker[b]	LOD Score[c]	R^{2d}	a^e
Cdtol-1	LG3-HMA4	9.87	42.9	−57.8085
Cdtol-2	LG4-ICE12	4.53	23.7	−45.7050
Cdtol-3	LG6-AthCDPK9	4.43	15.9	−37.0000

[a]QTL are named by the trait and ordered from 1 to 3. [b]LG on which QTL were mapped and marker at QTL position. [c]Maximum LOD score at the QTL position. [d]Percentage of explained variance of the QTL. [e]Additive effects of the QTL, corresponding to the differences between the Cd tolerance means (micromolars of Cd) of the two genotypic groups in the BC1 progeny (negative values imply that the *A. halleri* allele increases Cd tolerance compared to the *Alp* allele).

HMA4 Expression in the BC1 Parental Genotypes and Individuals

The expression of *HMA4* was studied by RT-PCR in the root and shoot of the BC1 parental genotypes *A. halleri*, *A. lyrata* sp. *petraea*, and the F1 individual with or without exposure to $CdSO_4$ (0 or 10 μM for 72 h, Fig. 5A; 100 μM for 72 h or 7 d for *A. halleri*, data not shown). The analysis was performed with primers designed in a perfectly conserved coding region between *AhHMA4* and *AlpHMA4* cDNAs.

HMA4 was highly expressed in the root and shoot of *A. halleri* and, to a lesser extent, in the root and shoot of the F1 individual. Almost no signal was detected in the root and shoot of the Cd-sensitive parental genotype *A. lyrata* sp. *petraea* at the same number of amplification cycles. Overall, *HMA4* was more highly expressed in the roots compared to the shoots. Four additional PCR cycles were needed to observe a band intensity in the shoots similar to the one obtained in roots. Transcript levels of *HMA4* were not affected by the Cd concentration (10 μM or 100 μM $CdSO_4$) or the duration (72 h or 7 d) of the treatment.

HMA4 expression was further studied in the roots of 21 BC1 genotypes distributed among eight different classes characterized by the presence or absence of the *A halleri* allele at one or more of the QTL for Cd tolerance (Fig. 5B). This analysis revealed that *HMA4* was highly expressed independently of the presence of the *A. halleri* allele at the QTL Cdtol-2 and Cdtol-3. Indeed, high expression levels of *HMA4* were obtained in the BC1 individuals harboring the *A. halleri* allele at the QTL Cdtol-1, while carrying two *A. lyrata* sp. *petraea* alleles at the QTL Cdtol-2 and Cdtol-3 (class 1). On the contrary, low expression levels, comparable to those observed in *A. lyrata* sp. *petraea* roots, were observed for the BC1 individuals belonging to classes 2 and 3, carrying the *A. halleri* allele at the QTL Cdtol-2 and Cdtol-3, respectively, and the *A. lyrata* sp. *petraea* alleles at the other QTL (Fig. 5B).

Role of AhHMA4 in Cd and Zn Tolerance and Transport in Yeast

To investigate the function of AhHMA4, the full-length and AhHMA4-C sequences were cloned in pYES2-GFP under control of the GAL1 promoter and expressed in the yeast strains BY4741 (wild type) and the Zn-sensitive *zrc1/cot1* double mutant. HMA4 inserts were also cloned without translational fusion with GFP. Growth tests were performed using two Cd and Zn concentrations depending on the yeast strain: 75 μM Cd and/or 10 mM Zn for BY4741 and 50 μM Cd and/or 10 mM Zn for *zrc1/cot1*. The expression of *AhHMA4* increased the sensitivity of BY4741 to Cd and Zn, whereas the expression of *AhHMA4-C* enhanced the tolerance of this strain to Cd and Zn (Fig. 6). Similar phenotypes were observed for *zrc1/cot1* (data not shown). Interestingly, on Gal medium, yeast cells expressing *AhHMA4* grew more slowly than the other constructs, even without Cd. Translational fusions of the AhHMA4 and AhHMA4-C constructs with GFP did not modify the phenotype of transformed yeast (Fig. 6). Replacement of D_{401} by a G in the phosphorylation site of AhHMA4 ($AhHMA4D_{401}G$) led to loss of the metal-sensitive phenotype, suggesting that this phenotype was due to transport activity (Fig. 6).

To confirm the expression of the recombinant proteins, immunoblots blots were performed on cytoplasmic and membrane fractions of transformed yeast (grown on Gal) using anti-GFP antibodies. In the membrane fraction (lanes 1 and 2) and in the soluble fraction (lane 3) of yeast extracts, proteins were detected of the correct predicted size (151.8 kD for AhHMA4:GFP and 73.9 kD for AhHMA4-C:GFP; Fig. 7). The size of the lower bands in the membrane

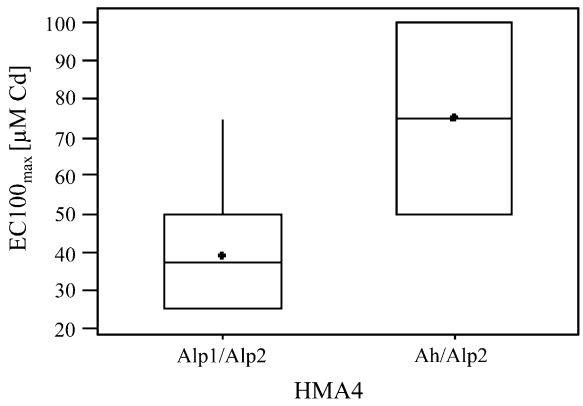

Figure 2. Box plot for Cd tolerance at the marker *HMA4,* located at the maximum LOD score position of the QTL Cdtol-1. Box plots for Cd tolerance are given for two groups of BC1 individuals that can be distinguished based on their genotype at the marker *HMA4,* i.e. those carrying both alleles from the nontolerant parental individuals *A. lyrata* sp. *petraea* 1 and *A. lyrata* sp. *petraea* 2 at the three QTL or markers *HMA4, ICE12,* and *AthCDPK9* and those carrying one allele from the tolerant parental individual *A. halleri* and one from the nontolerant parental individual *A. lyrata* sp. *petraea* 2 at the marker *HMA4,* while carrying both alleles from the nontolerant parental individuals *A. lyrata* sp. *petraea* 1 and *A. lyrata* sp. *petraea* 2 at the markers *ICE12* and *AthCDPK9* ($P = 0.001$). The boxes represent the interquartile range, with arithmetic means indicated by black diamonds and medians indicated by horizontal lines. Whiskers connect the nearest observations within 1.5 times the interquartile ranges of the lower and upper quartiles.

Table II. *Epistatic interactions between QTL for Cd tolerance*

Source	df[a]	On Raw $EC100_{max}$ Data				On Log-Transformed $EC100_{max}$ Data			
		SS[b]	MS[c]	F[d]	P[e]	SS[b]	MS[c]	F[d]	P[e]
Cdtol-1	1	46,465	46,465	75.87	0	1.42009	1.42009	70.37	0
Cdtol-2	1	17,030	17,030	27.81	0	0.55831	0.55831	27.67	0
Cdtol-3	1	12,967	12,967	21.17	0	0.30622	0.30622	15.18	0
Cdtol-1 × Cdtol-2	1	709	709	1.16	0.286	0.01897	0.01897	0.94	0.336
Cdtol-1 × Cdtol-3	1	3,379	3,379	5.52	0.022	0.02255	0.02255	1.12	0.294
Cdtol-2 × Cdtol-3	1	503	503	0.82	0.368	0.00009	0.00009	0	0.947
Error	69	42,260	612			1.39236	0.020179		
Total	75	144,178				4.59379			

[a]Degrees of freedom. [b]Sum of squares. [c]Mean squares. [d]Values of F statistic. [e]Significance levels.

extracts of *AhHMA4*-expressing cells most probably corresponds to degradation products.

Measurements of intracellular Cd indicated reduced accumulation of Cd in yeast overexpressing *AhHMA4* compared to yeast cells transformed with empty plasmid (Fig. 8). No difference in Cd content was observed between cells expressing *AhHMA4-C* or *AhHMA4D$_{401}$G* compared to cells transformed with the empty vector.

Localization of AhHMA4 in Yeast and in Planta

Because the expression of AhHMA4-GFP and AhHMA4-C-GFP fusion proteins in yeast cells gave a similar phenotype to the GFP unfused proteins, we used GFP to investigate the subcellular localization of HMA4. At the standard image acquisition settings used for GFP visualization, autofluorescence from cells transformed with the untagged *AhHMA4* was absent (data not shown), so all detectable fluorescence in the transformants was GFP specific. When exponentially growing cells were analyzed, green fluorescence resulting from the expression of *AhHMA4*:*GFP* and *AhHMA4 D$_{401}$G:GFP* showed a ring-like pattern around the cells and the nucleus (Fig. 9). AhHMA4-C:GFP was only visible in the cytosol. To verify the absence of the fused proteins in the tonoplast, this membrane was stained for a short term with the lipophilic dye FM4-64, which selectively stains yeast vacuolar membrane (Vida and Emr, 1995). Superposition of the GFP and FM4-64 images demonstrated the absence of detectable GFP fused protein in the tonoplast (Fig. 9).

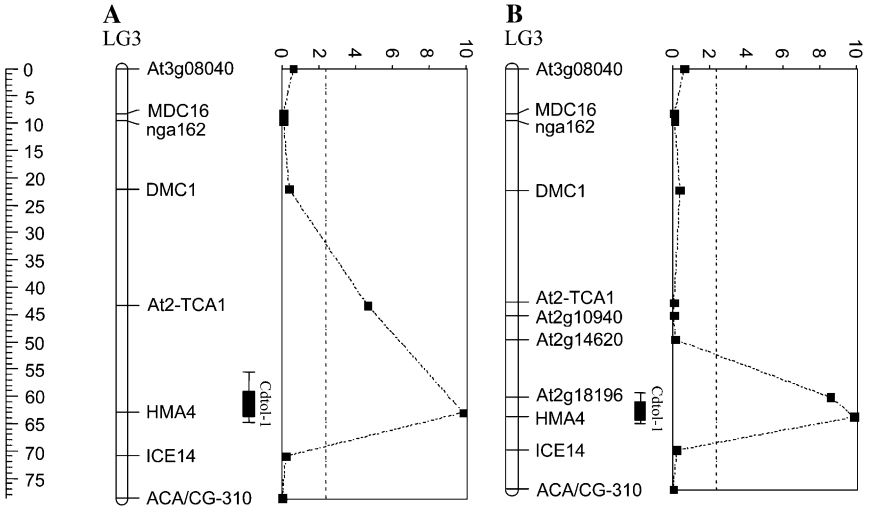

Figure 3. Densification of the major QTL region Cdtol-1. A, LG LG3, on which initially eight markers were mapped, is represented. The position in centiMorgans of the markers on LG3 is given by the ruler. The LOD score profile along the LG is represented at the right of the LG. Map positions are plotted along the vertical axis and LOD scores are plotted along the horizontal axis. Dashed lines correspond to the LOD score threshold (2.4) for QTL detection at an error level $\alpha = 0.05$. The position of a QTL is shown as the interval over which the LOD score is within one or two log units of its maximum value, i.e. at the most likely position of the QTL. Bars indicate the one-LOD (10-fold) support interval and whiskers (lines extending beyond bars) indicate the two-LOD (100-fold) support intervals. The length of the one- and two-LOD support intervals correspond to approximately 5 and 9 cM, respectively. B, Three additional markers *At2g10940*, *At2g14620*, and *At2g18196* were mapped on LG3 to increase the accuracy of the major QTL position. A reduction in length of the LOD support intervals associated with the QTL Cdtol-1 was obtained: one- and two-LOD support intervals correspond to approximately 4 and 6 cM, respectively.

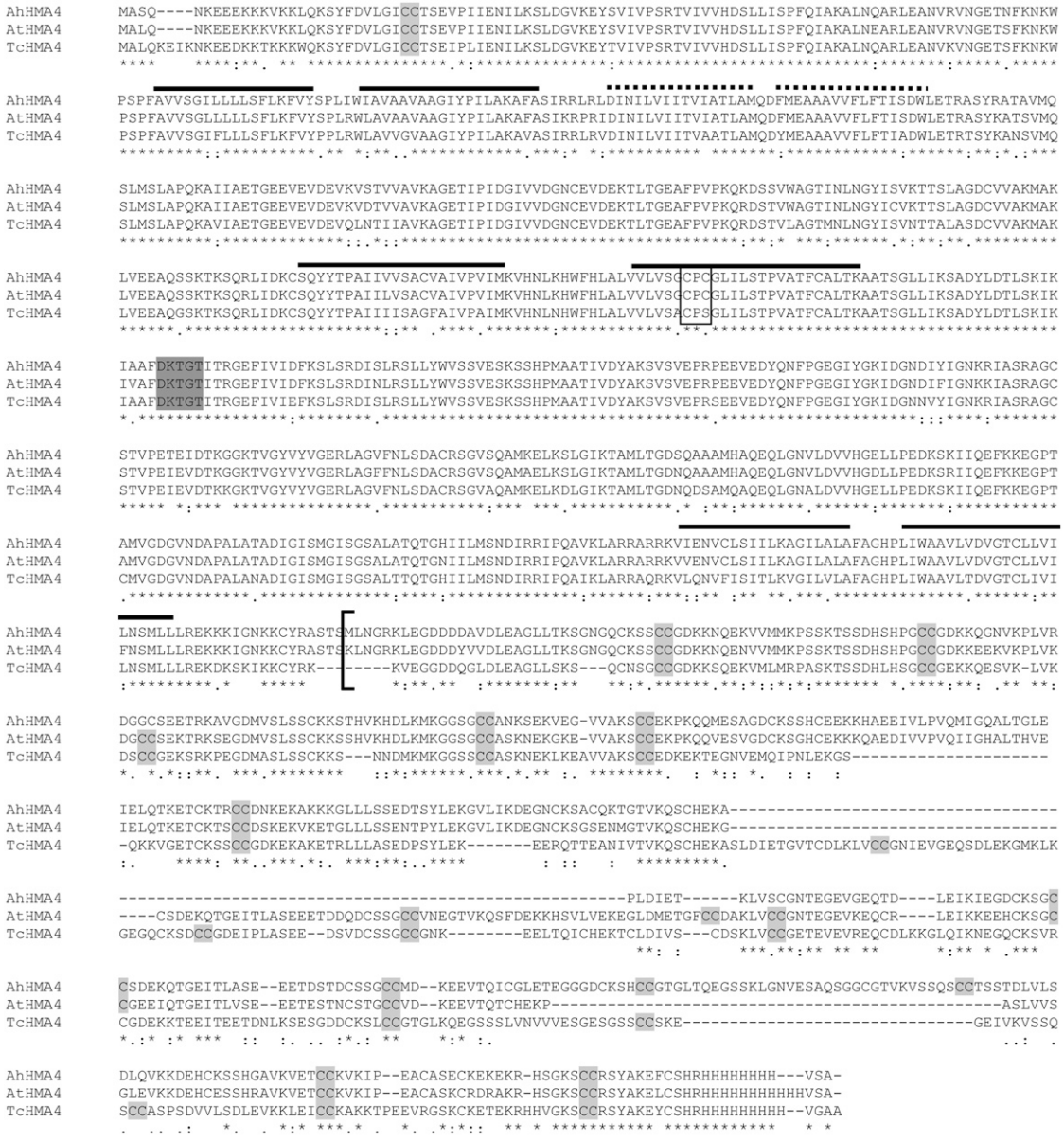

Figure 4. Sequence similarity of AhHMA4 (Auby, France) to other HMA4 amino acid sequences. Deduced amino acid sequences for AhHMA4 (accession no. DQ221101), AtHMA4 (NM127468), and TcHMA4 (AJ567384) are shown aligned using the ClustalW method (Thompson et al., 1994). A number of motifs common to P_{1B}-type ATPases are indicated, including the highly conserved CPx motif (boxed), the ATPase phosphorylation site (shaded in dark gray), the transmembrane spans (consensus: continued lines; probable: dotted lines, according to ARAMEMNON predictions softwares). Also, Cys residues in the C terminus are highlighted. The start of the C-terminal fragment used in the yeast tolerance assay is indicated with a bracket. Asterisks (*) indicate the identical residues; ":" indicates that one of the following strong groups is fully conserved: STA, NEQK, NHQK, NDEQ, QHRK, MILV, MILF, HY, and FYW; "." indicates that one of the following weaker groups is fully conserved: CSA, ATV, SAG, STNK, STPA, SGND, SNDEQK, NDEQHK, NEQHRK, FVLIM, and HFY.

The AhHMA4:GFP fusion protein was transiently overexpressed in tobacco (*Nicotiana tabacum*) epidermal cells, which were then analyzed by confocal laser scanning microscopy. The superposition of the bright-field image and the corresponding fluorescence image showed an unambiguous localization of GFP to the plasma membrane (Fig. 10).

DISCUSSION

QTL Analysis of Cd Tolerance in *A. halleri*

Three QTL for Cd tolerance were detected in the *Ah* × *Alp* BC1 progeny through MQM. These QTL explained the major part of the phenotypic (82.5%) and genetic variance (92.7%) observed for this trait in the mapping

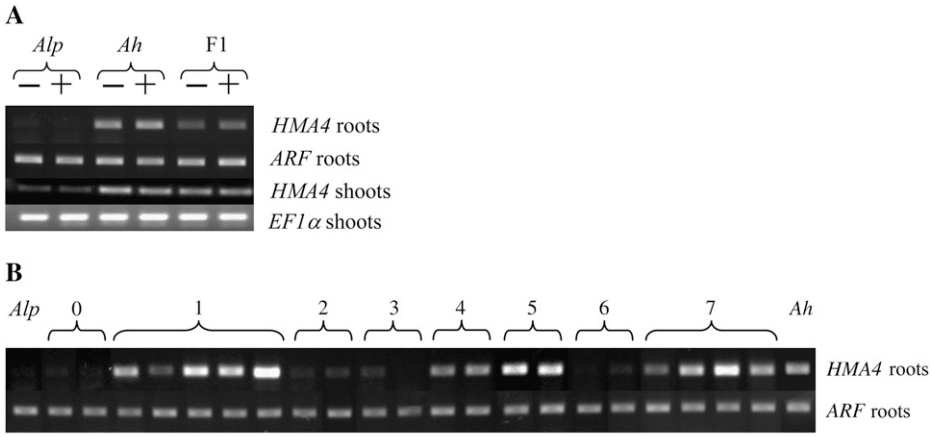

	A. halleri allele at		
Group	Cdtol-1	Cdtol-2	Cdtol-3
0			
1	X		
2		X	
3			X
4	X	X	
5	X		X
6		X	X
7	X	X	X

Figure 5. RT-PCR analysis of *HMA4* on *A. halleri, A. lyrata* sp. *petraea,* F1, and BC1 progeny. A, RT-PCR was used to compare transcript levels for *HMA4* or *EF1α* (as a control) in roots and shoots of *A. halleri, A. lyrata* sp. *petraea,* and the F1 individual. Plants were grown on hydroponic media containing 0 (−) or 10 μM $CdSO_4$ (+) for 72 h. The PCR conditions were the same for *HMA4* in roots and *EF1α* in roots and in shoots (24 cycles), but 29 cycles were used to detect *HMA4* expression in shoots. B, RT-PCR was used to compare transcript levels of *HMA4* or *ARF* (as a control) in roots of *A. halleri, A. lyrata* sp. *petraea,* and 21 BC1 individuals belonging to eight different classes characterized by the presence or the absence of an *A. halleri* allele at one, two, or three QTL for Cd tolerance. Plants were grown on hydroponic media. Amplification was performed for 24 cycles for *HMA4* and 20 cycles for *ARF*. The table represents the different groups of the BC1 individuals based on the presence or the absence of an *A. halleri* allele at one, two, or three QTL for Cd tolerance. The presence of the *A. halleri* allele at the QTL Cdtol-1, Cdtol-2, and/or Cdtol-3 is indicated by X.

population. However, some caution should be adopted in the interpretation of this result. Due to the relatively small progeny size (<100 individuals), as well as the segregation distortion observed at the QTL Cdtol-3 (markers *ICE2* and *AthCDPK9*), QTL of minor effect probably remained undetected and the effects of the detected QTL might be overestimated (Beavis et al., 1994; Bradshaw et al., 1998).

Genetic Architecture of Cd Tolerance in *A. halleri*

The genetic architecture of Cd tolerance was previously addressed by Bert et al. (2003) through the analysis of the segregation of Cd tolerance in 66 of the 79 BC1 individuals used in this QTL experiment. The segregation ratios were shown to be significantly different from the 1:1 ratio expected for a character controlled by a single major gene, while the hypothesis of Cd tolerance controlled by two or three major genes with additive effect could not be rejected (Bert et al., 2003). The QTL analysis performed in this study provided evidence for the involvement of one major QTL explaining almost half (48.2%) of the genetic variance observed for Cd tolerance in the BC1 progeny, and two QTL of less major effect on Cd tolerance. As we did not detect any significant epistatic interaction between the QTL, the three QTL presumably have a largely additive effect. At all three QTL, the trait-enhancing allele was found to originate from the Cd-tolerant parental genotype *A. halleri*. The *A. halleri* individual used in this study originated from an industrial polluted site characterized by elevated concentrations of Zn, Cd, and Pb (Van Rossum et al., 2004). The high selective pressures represented by the occurrence of toxic ambient Cd concentrations most probably led to the selection of genes increasing Cd tolerance, which should give rise to the positive effect on Cd tolerance of the *A. halleri* alleles (Orr, 1998). Whereas this explanation is plausible for metallicolous *A. halleri* individuals, it remains to be verified for

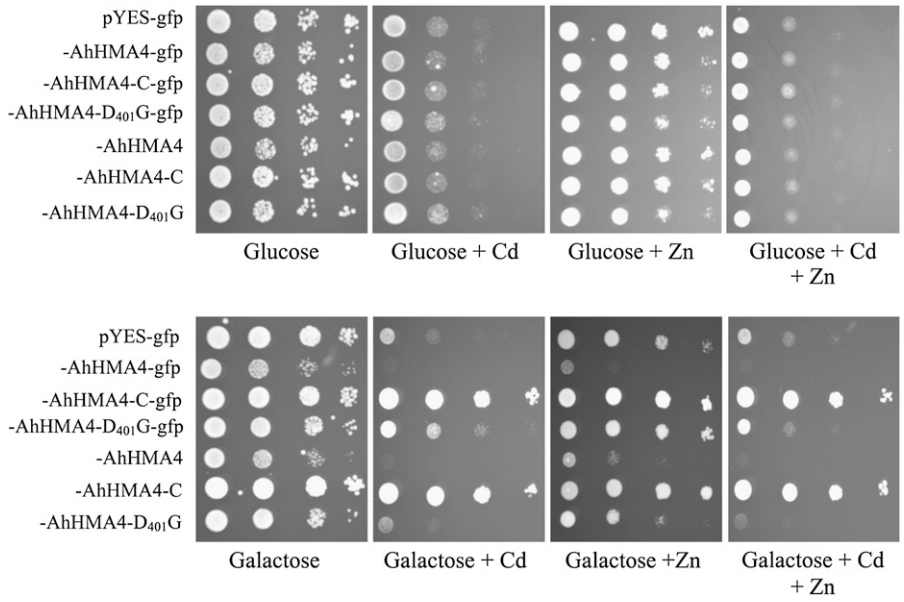

Figure 6. Growth of yeast strain BY4741 on selective media. Yeast cells were transformed with the empty pYES2-GFP vector, with the full-length AhHMA4 sequence, with the C-terminal sequence, or with the AhHMA4-D_{401}G sequence fused or not with GFP at the C-terminal end. Yeast cells were grown in SD induction medium to an OD_{600} of 1.0, serially diluted to an OD_{600} of 0.1 to 0.0001 (from left to right in each section), and then 10 μL drops spotted on plates containing Glc or Gal and 0 or 75 μM of $CdSO_4$ and 0 or 10 mM $ZnSO_4$. Plates were incubated for 5 d at 30°C. Drop tests were repeated at least three times with similar results.

A. halleri individuals growing on unpolluted sites, which are not subject to a high selective pressure for Cd tolerance.

The *A. halleri* origin of the trait-enhancing allele at all three QTL might indicate the constitutive presence of Cd tolerance in *A. halleri*, as observed for Zn tolerance (Bert et al., 2002; Pauwels et al., 2006). However, this should be confirmed through an extensive survey of Cd tolerance in metallicolous and nonmetallicolous *A. halleri* populations. Interestingly, the genetic architecture of Zn tolerance, studied through a QTL analysis on the same mapping population, revealed three QTL for Zn tolerance, among which one showed colocalization with the major QTL Cdtol-1 for Cd tolerance. The involvement of this QTL in both metal tolerances might indicate that Cd and Zn tolerance initially evolved in *A. halleri* through the fixation of the QTL conferring tolerance to both metals (Willems et al., 2007).

Cloning and Analysis of *AhHMA4* Expression

The *HMA4* locus was located at the peak of the major QTL region for Cd tolerance in the *Ah* × *Alp* BC1 progeny. In silico analysis of the full-length coding sequence of *AhHMA4* did not reveal common features between the sequences of AhHMA4 and TcHMA4 that could differentiate these metal-tolerant species from Arabidopsis. Rather, the HMA4 sequences of *A. halleri* and Arabidopsis were most similar to each other, reflecting the phylogenetic relatedness of these taxa. Indeed, although the Cys- and His-rich C terminus of HMA4 may play a role in metal chelation or regulation of activity, the positions of these potential metal-binding residues were not more highly conserved between the Cd/Zn hyperaccumulator species *A. halleri* and *T. caerulescens* than between *A. halleri* and Arabidopsis. This might indicate that rather than their position, the presence of these potential metal-binding residues is important.

HMA4 was more highly expressed in the roots and shoots of *A. halleri* than in *A. lyrata* sp. *petraea* or, to a lesser extent, the F1 individual. Moreover, in the BC1 progeny the presence of the *AhHMA4* allele was always accompanied by a higher *HMA4* expression even in the absence of the *A. halleri* allele at the QTL Cdtol-2 and Cdtol-3. No significant modification of *HMA4* expression level was observed in *A. halleri* or in the F1

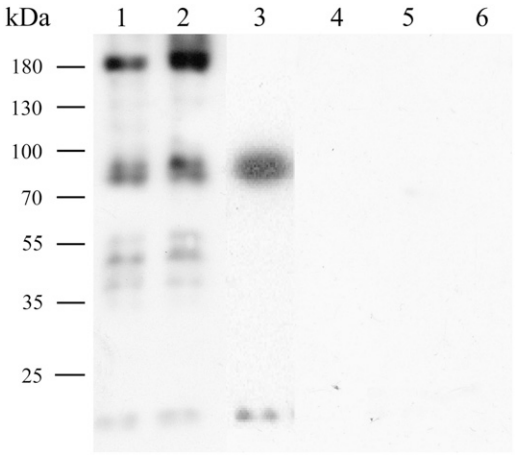

Figure 7. Western-blot analysis of GFP fusion proteins. Yeast containing pYES2-GFP vector (1 and 5) or expressing either the AhHMA4:GFP (2 and 6), the AhHMA4-D_{401}G:GFP (3 and 7), or the AhHMA4-C:GFP (4 and 8) fusion protein were grown on medium with 2% Gal (1–4) or with 2% Glc (5–8). Proteins were extracted (membrane proteins: 2, 3, 6, and 7; soluble proteins: 1, 4, 5, and 8) and separated on 8% SDS-PAGE gels and further analyzed using anti-GFP antibodies. Numbers beside the gel indicate molecular mass in kilodaltons.

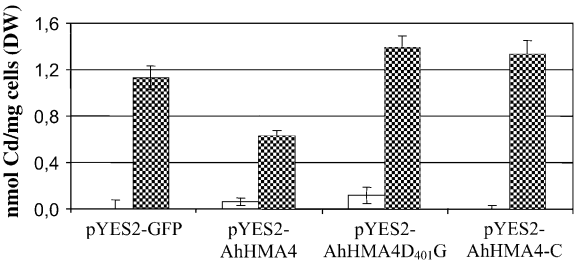

Figure 8. Cd content in BY4741 expressing AhHMA4, AhHMA4D$_{401}$G, or AhHMA4-C. Yeast BY4741 cells transformed with the pYES2-GFP plasmid and with the pYES2-GFP containing AhHMA4, AhHMA4G$_{401}$D, or AhHMA4-C were grown in liquid SD induction media with (hatched bars) or without 20 μM $CdSO_4$ for 48 h (white bars). Metal contents were analyzed by atomic absorption spectroscopy. Results are an average (±SE) from three independent experiments.

individual upon exposure to increased Cd concentrations or upon prolonged exposure to Cd.

In *A. halleri*, a higher expression of *HMA4* was recently reported and suggested to be related to the presence of several copies of this gene in the *A. halleri* genome (Talke et al., 2006). In this work, the amplification of *HMA4* for its mapping on the *Ah* × *Alp* genetic linkage map revealed a single fragment in *A. halleri* different in size from the one amplified in *A. lyrata* sp. *petraea*. Consequently, only one locus was mapped on the *Ah* × *Alp* linkage map, which was located on its expected position based on the synteny of the *Ah* × *Alp* map with the Arabidopsis genome. If all copies were located in a small region, this result would not be not in contradiction with the hypothesis of the presence of several copies of *HMA4* in the *A. halleri* genome. Such genomic amplification could be explained by a duplication event at the same locus in *A. halleri*.

Role of HMA4 in Metal Transport: Functional Expression in Yeast and Localization in Yeast and Plant Cells

To address the critical question of the physiological function of HMA4, both in vivo and in vitro metal transport studies were performed and showed that P_{1B}-ATPases drive the export of ions from the cell cytoplasm (Eren and Arguello, 2004). Another approach, which was undertaken to characterize HMA4, consisted of the functional expression of HMA4 in yeast. Heterologous expression of *AtHMA4* in yeast resulted in an increased tolerance to Cd (Mills et al., 2003), but increased (or did not alter) also the sensitivity to Zn, Co, Cu, or nickel (Verret et al., 2005). AtHMA4:GFP fusion protein was observed essentially in endocytic vesicles and to a lesser extent at the plasma membrane (Verret et al., 2005). Enhanced Cd tolerance was also observed in yeast cells transformed with *TcHMA4* (Papoyan and Kochian, 2004). On the contrary, Bernard et al. (2004) expressed *TcHMA4* as well as *AtHMA4* in two different wild-type yeast strains and observed a higher sensitivity to high Zn and Cd concentrations.

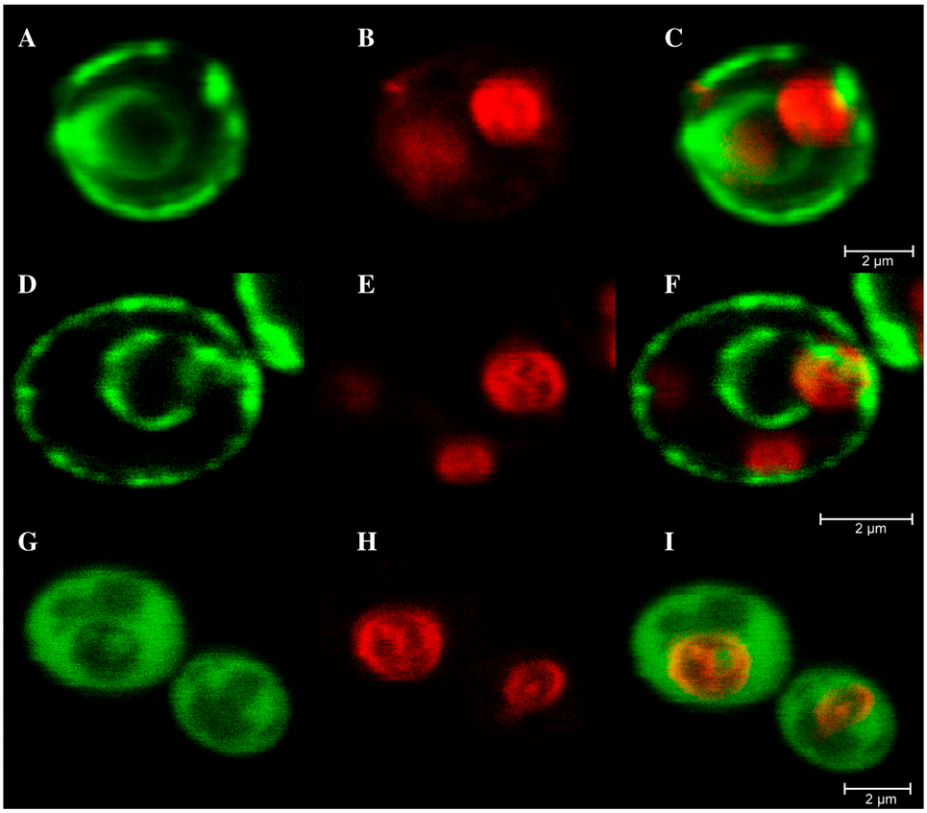

Figure 9. Localization of AhHMA4:GFP, AhHMA4D$_{401}$G:GFP, and AhHMA4-C:GFP fusion proteins in yeast, viewed by confocal laser scanning microscopy. Cells were visualized after 20 h of induction. Three images from the same cell are shown. A, GFP fluorescence from a AhHMA4:GFP-expressing strain. B, FM4-64 staining the vacuolar membrane of the same cell. C, A pseudocolored merged image with GFP in green and FM4-64 in red. D, E, and F and G, H, and I are as for A, B, and C, but expressing the AhHMA4D$_{401}$G:GFP and AhHMA4-C:GFP proteins, respectively. Bars = 2 μM.

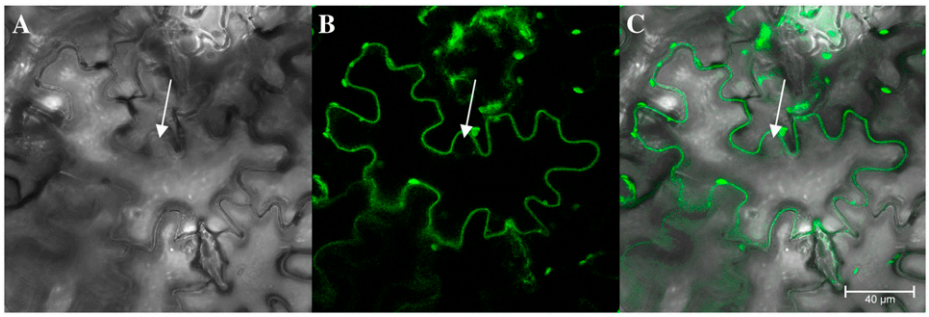

Figure 10. Plasmalemma localization of the AhHMA4:GFP fusion protein in tobacco plants, viewed by confocal laser scanning microscopy. Transient expression of AhHMA4:GFP in tobacco leaf epidermal cells. A, Bright-field image of the tobacco leaf epidermis. The nucleus is indicated with an arrow. B, GFP fluorescence in the same cell concentrated to the plasmalemma, which followed the cell contour, outside the nucleus. C, Pseudocolored merged image with GFP in green. Bar = 40 μM.

In this work, heterologous expression of *AhHMA4* in yeast resulted in an increased sensitivity to Cd and Zn. A mutation in the conserved phosphorylated Asp of AhHMA4 restored the capacity of growth of the strains in presence of high Zn and Cd concentrations, indicating that the higher sensitivity to Zn and Cd was related to a transport activity (ATP hydrolysis coupled to transport activity). The sensitivity of yeast upon *HMA4* overexpression might be due to the transport of metals not only to the outside of the cells, but also from the cytoplasm to metal-sensitive organelles due to the lack of a specific targeting sequence for yeast. The first transport process would result in the reduced metal content while the second would be responsible for the sensitive phenotype. Our hypothesis is supported by the localization of GFP-tagged AhHMA4 at the plasma membrane as well as at the endoplasmic reticulum (ER) around the nucleus in the yeast. In agreement with this, immunoblot analysis of AhHMA4 indicated a good translation and accumulation of the protein. Strong evidence for the high sensitivity of the ER to Cd accumulation was previously published by Clemens et al. (2002), who showed that the *zhf* deletion mutant of *Schizosaccharomyces pombe*, impaired

Table III. *List of primers used with their positions (base pair) on At2g10940, At2g14620, At2g18196, AhHMA4, EF1α, and ARF sequences in order of their first mention in ''Materials and Methods''*

Restriction sites are underlined. Lowercase letters in primers AhHMA-ATPXF and AhHMA-ATPXR indicate the mismatched nucleotides designed for specific mutations.

Name	Sequences (5′-3′)	Positions
At2g10940F	AAGCTACCCGTTCCTCC	351–367
At2g10940R	CGACTTCAACGAGGCCTTTA	794–813
At2g14620F	CACAAGCTTCCGTTGTTTCA	188–207
At2g14620R	ATGGACCCTTTGACCAATCA	751–769
At2g18196F	ATGCCAATGGCTCGTCCACT	106–125
At2g18196R	CACATCCACTGCAACACATC	156–175
EF1αF	ATTGTGGTCATTGGCCACGTCGA	27–50
EF1αR	CTCCTTCTCAATCTCCTTACCAG	1,191–1,214
AtTcHMA4F	TGACCTGAAAATGAAAGGTGGTTC	2,474–2,498
AtTcHMA4R	TGCATAACTCCTGCAACAGCT	3,237–3,258
AhHMA3′RACE	AGCTGTTGCAGGAGTTATGCA	3,408–3,429
AhHMA5′RACE	CTCGAGGGAACGATGACGG	145–164
AhHMA4F	CCAAGCTTATGGCGTCACAAAACAAAGAAG	1–22
AhHMA4R	CGGATCCTCAAGCACTCACATGGTGATG	3,465–3,483
AhHMA4nostpR	CCGGATCCCCAGCACTCACATGGTGATGGG	3,463–3,480
AhHMA4C	CCAAGCTTATGTTGAATGGTAGGAAACTCG	2,160–2,182
AhHMA-ATPXF	TTCGgCCAAACCGGGACTATTACC	1,197–1,221
AhHMA-ATPXR	GTTTGGcCGAAAGCAGCGATTTTGA	1,183–1,208
AhHMA4BamF	CCGGATCCATGGCGTCACAAAACAAAGAAG	1–22
AhHMAKpnR	CCGGTACCAGCACTCACATGGTGATGGG	3,463–3,480
ARF_F	GGTCTCGATGCAGCTGGTAAGACTAC	177–202
ARF_R	TGTTAGAGAGCCAGTCAAGTCCCTCA	608–633
HMA4_290F	TAGTGGCAAAGAGCTGTTGTGA	2,537–2,558
HMA4_290R	TGCAGTTTCCTTCATCTTTAATCAG	2,800–2,825

in an ER-localized cation diffusion facilitator transporter capable of transporting Cd into this organelle, was more tolerant to Cd than the wild type. This suggests that Cd ions may exert their toxic effects on cellular metabolism in the ER.

In plant cells, however, the AhHMA4-GFP fusion was only detected in the plasma membrane, consistent with a role in metal detoxification by export from the cell. This localization was previously reported for AtHMA4 (Verret et al., 2005).

Conclusion: Role of HMA4 in Metal Tolerance

In Arabidopsis, *HMA4* is mainly expressed in the vascular tissues of roots, leaves, and stems (Hussain et al., 2004; Verret et al., 2004). Analysis of *hma4* null mutant lines revealed an increased sensitivity to Zn and Cd (Verret et al., 2004; Mills et al., 2005), as well as a decreased Zn and Cd accumulation in shoot tissues when compared to the wild type under high Zn concentrations (Hussain et al., 2004; Verret et al., 2004). On the contrary, AtHMA4-overexpressing plants had an increased tolerance to high Zn and Cd, as well as higher Cd and Zn levels in the leaves compared to the wild type. Based on these results, a role of HMA4 was proposed in the root-to-shoot translocation of Cd and Zn, in the redistribution of metals in the whole plant, and in the detoxification of the cytosol through the exclusion of metals from sensitive cells by acting as an efflux pump (Hussain et al., 2004; Verret et al., 2004; Mills et al., 2005). Up to now, experimental data suggest that HMA4 transports free metal ions, probably delivered to HMAs in a coordinated form, but by means that remain currently unknown (Eren and Arguello, 2004; Verret et al., 2005).

In the Cd/Zn hyperaccumulators *A. halleri* and *T. caerulescens* (Bernard et al., 2004), *HMA4* is more highly expressed in both roots and shoots compared with Cd/Zn-sensitive close relatives. The elevated expression of *HMA4* in two different Zn/Cd hyperaccumulator species that evolved independently strongly supports the idea that HMA4 plays an important role in tolerance to both metals. In *A. halleri* at least, this hypothesis is reinforced by the QTL analysis of Cd (this study) and Zn tolerance (Willems et al., 2007) performed on the *Ah* × *Alp* BC1 progeny, indicating the colocalization of the QTL Cdtol-1 and Zntol-1, both of which are located at the marker *HMA4* on the *Ah* × *Alp* linkage map. As observed in AtHMA4-overexpressing lines (Verret et al., 2004), the increased expression of *HMA4* in *A. halleri* or *T. caerulescens* might be related to the increased Cd and Zn tolerance and hyperaccumulation phenotype of these species. However, we cannot exclude the possibility that the activity of HMA4 proteins also displays different characteristics or differential regulation in Arabidopsis and the hyperaccumulator species.

In this work, we have shown that in addition to the major QTL Cdtol-1 at least two other QTL are involved in Cd tolerance in *A. halleri*. Among the candidate genes responsible for metal tolerance in *A. halleri*, MTP1 was reported to be capable of transporting Zn into the vacuole and two of the three *MPT1* copies present in *A. halleri* were shown to cosegregate with Zn tolerance (Dräger et al., 2004; Willems et al., 2007). However, none of these copies colocalized with the QTL for Cd tolerance. Consequently, *HMA4* is currently the only gene for which there is genetic evidence for a role in both Zn and Cd tolerance.

Taken together, all available data point to the elevated expression of HMA4 P_{1B}-type ATPase as an efficient mechanism for improving Cd/Zn tolerance in plants under conditions of Cd/Zn excess by maintaining low cellular Cd^{2+} and Zn^{2+} concentrations in the cytoplasm.

MATERIALS AND METHODS

Plant Material, Growth Conditions, and Treatments

A cross was performed between an individual of the Zn/Cd-tolerant *Arabidopsis halleri* sp. *halleri* species (pollen donor), collected on a site highly contaminated with Zn, Cd, and Pb (Auby, France [Van Rossum et al., 2004]), and an individual of the nontolerant *Arabidopsis lyrata* sp. *petraea* (*Alp*) species (pollen recipient; Unhost, Central Bohemia, Czech Republic [Macnair et al., 1999]). To obtain a first-generation backcross (BC1) progeny, one randomly chosen F1 individual was crossed with a second *A. lyrata* sp. *petraea* individual (pollen recipient; Unhost, Central Bohemia, Czech Republic; Bert et al., 2003).

Cuttings from mother plants were grown on sand for 6 weeks in a glasshouse (light and humidity conditions changed according to the season, the temperature being kept above 5°C at night in winter). Hydroponic plant culture was performed in a modified Murashige and Skoog solution consisting of K_2SO_4 (0.88 mM), KH_2PO_4 (0.25 mM), NaCl (10 μM), $Ca(NO_3)_2$ (2 mM), $MgSO_4$ (1 mM), FeEDDHA (20 μM), H_3BO_3 (10 μM), $ZnSO_4$ (1 μM), $MnSO_4$ (0.6 μM), $CuSO_4$ (0.1 μM), and $(NH_4)_6Mo_7O_{24}$ (0.01 μM), adjusted to pH 5.8 in a climate-controlled growth chamber (temperature cycle of 20°C/17°C and a light [100 μmol m^{-2} s^{-1}] cycle of 16 h light/8 h dark). The hydroponic solutions used were continuously aerated and changed every week. After 6 weeks in nutrient solution, 10 μM $CdSO_4$ was added. Roots and shoots were collected after 72 h or 7 d of treatment and immediately frozen in liquid nitrogen until use.

Phenotypic Evaluation of Cd Tolerance

Cd tolerance was assessed on 79 individuals of the *A. halleri* × *A. lyrata* sp. *petraea* BC1 progeny. Two to three clonal replicates of each BC1 individual were obtained through vegetative propagation. After growth for 6 weeks on sand moistened with deionized water, rooted cuttings were transferred to 4 L vessels containing a nutrient solution to which Cd was added as $CdCl_2$. To measure Cd tolerance, plants were sequentially transferred to increasing concentrations of Cd. The range of Cd concentrations tested was 10, 25, 50, 75, 100, 150, and 250 μM (Bert et al., 2003). At the end of each week, roots of each plant were gently dried with tissue paper and the whole plant was weighed. In addition, root length was measured. Cd tolerance was determined as the lowest concentration at which no new root growth was observed (the EC100; Bert et al., 2003).

QTL Mapping of Cd Tolerance

Statistical Analysis

The genotype effect of Cd tolerance in the BC1 progeny was estimated by a one-way ANOVA using the generalized linear model procedure in SAS (SAS, 1999). The broad-sense heritability of this trait was calculated using the mean square values (MS) of ANOVA analysis ($h^2 = MS_{genot}/[MS_{genot} + MS_{error}]$). Type III sums of squares were used because the data set was unbalanced due to the unequal number of replicates of each BC1 individual. We performed an Anderson-Darling test (Minitab) on the $EC100_{max}$ values (the maximum value of the EC100 values of the clones) of the BC1 genotypes to test for deviation

from a normal distribution. We tested for significant pairwise interactions between the QTL using the generalized linear model procedure in Minitab. The markers at the QTL position were considered as fixed factors in this analysis. The box plot for Cd tolerance at the marker *HMA4* was obtained using Minitab. We performed a Kruskal-Wallis test, based on Wilcoxon rank scores of the data, to test for significant differences of Cd tolerance between both groups (Minitab).

QTL Analysis

The set of markers (65 Arabidopsis [*Arabidopsis thaliana*]-anchored markers and 18 amplified fragment length polymorphism markers) and the genetic map of the *Ah* × *Alp* BC1 progeny (henceforth called the *Ah* × *Alp* map) obtained with the program Joinmap 3.0 (Van Ooijen and Voorips, 2001; Willems et al., 2007) were used for the QTL analysis of Cd tolerance, performed with the MapQTL 4.0 program (Van Ooijen et al., 2002). QTL of Cd tolerance were identified using $EC100_{max}$ values of the BC1 genotypes. The significance threshold of the LOD score for QTL detection was obtained by performing a permutation test on the quantitative data and set at a LOD score of 2.4, corresponding to an error level $\alpha = 0.05$. A first QTL analysis was performed using interval mapping (IM). In IM, LOD scores were calculated every centiMorgan (cM) within the intervals along the LGs. The markers for which the LOD score exceeded the significance threshold were included in an automatic cofactor selection analysis and the selected markers were then used as cofactors in MQM analysis. In MQM mapping, a one-dimensional search over the genome is performed as in IM, while simultaneously fitting the selected cofactors that take over the role of the other QTL. In the QTL analysis of Cd tolerance, MQM mapping was performed twice while adjusting the set of cofactors to obtain the best possible set of QTL, i.e. showing maximal LOD scores. One- and two-LOD support intervals were obtained using Mapchart 2.1 (Voorrips, 2002). The percentage of variance explained by each QTL (R^2) was calculated in IM. Additive genetic effects correspond to the differences between the mean Cd tolerance levels of the BC1 individuals characterized by homospecific (i.e. *Alp*1/*Alp*2) and heterospecific (i.e. *Ah*/*Alp*2) allelic combinations at each QTL.

Marker Densification the Major QTL Region

Three additional markers (*At2g10940*, *At2g14620*, and *At2g18196*) selected using their position in the Arabidopsis genome, were mapped to increase the accuracy of the major QTL position. One primer was designed in an exonic region of the gene and the second primer was placed in the following exon (Table III). To obtain labeled PCR products detectable on the automated genotyper Li-Cor 4200 (Li-Cor-ScienceTec), the forward and reverse primer contained a 5′ tail of 19 bp (forward primer) or 20 bp (reverse primer) homologous to the universal consensus M13 primer sequence, followed by the locus-specific sequence (Oetting et al., 1995). The following PCR conditions were applied: PCR reactions were carried out in a total volume of 15 μL containing 20 ng of template DNA, 2 mM $MgCl_2$, 0.2 mg/mL bovine serum albumin, 0.2 mM dNTP, 0.15 μM of each M13 fluorescently labeled primer (either IRD-700 or IRD-800), 20 mM Tris-HCl (pH 8.3), 50 mM KCl, and 0.4 units of AmpliTaq DNA Polymerase (Applied Biosytems). PCR was performed on a Perkin-Elmer Gene-Amp system 9700: 94°C for 5 min, followed by locus-specific amplification: 94°C for 30 s, annealing temperature for 45 s, 72°C for 40 s (except for marker *At2g18196*: 72°C for 1 min 15 s), for eight cycles, followed by M13 labeling amplification: 94°C for 30 s, 50°C for 20 s, 72°C for 40 s, for 30 cycles, and a final extension 72°C for 7 min. The annealing temperature of the locus-specific cycles corresponded to 52°C, 48°C, and 58°C for the markers *At2g10940*, *At2g14620*, and *At2g18196*, respectively. Length polymorphisms of the markers *At2g10940* and *At2g18196* were revealed on polyacrylamide gels using a Li-Cor genotyper. For cleaved-amplified polymorphic sequence marker *At2g14620*, restriction was carried out in a total volume of 20 μL containing 10 μL of PCR product, 0.2 mM spermidine, 1× specific enzyme buffer provided by the supplier, and 1 unit of restriction enzyme *Alu*I. Restriction was carried out by incubation for at least 4 h at the appropriate temperature in a Perkin-Elmer Gene-Amp system 9700. The polymorphism was revealed on agarose gels.

Yeast Cultures, Transformation, and Growth Assays

The yeast (*Saccharomyces cerevisiae*) strains used for the heterologous expression of AhHMA4 were BY4741 (*MATa*, *his3*Δ1, *leu2*Δ0, *met15*Δ0, and *ura3*Δ0) obtained from Euroscarf (http://www.uni-frankfurt.de/fb15/mikro/euroscarf/) and the *zrc1/cot1* mutant (*Mat a*, *zrc1*::*natMX3*, *cot1*::*kanMX4*, *his3*Δ1, *leu2*Δ0, *met15*Δ0, and *ura3*Δ0) provided by U. Krämer (Golm, Germany). Yeast cells were transformed as described elsewhere (Gietz and Woods, 2002). They were grown at 30°C in yeast potato (*Solanum tuberosum*) dextrose or in synthetic defined (SD) medium (0.17% yeast nitrogen base [Sigma]) without amino acids, containing 1% (w/v) Glc or 2% (w/v) Gal (induction medium), supplemented with yeast synthetic dropout without uracyl (Sigma), pH 5.3. For metal tolerance assays, yeast was grown on SD medium (with 2% [w/v] Gal) to an OD_{600} of 1 to perform further dilutions. The drop assays were performed on SD plates containing 50 μM $CdSO_4$ for *zrc1/cot1* mutants and 75 μM for BY4741 with or without 10 mM $ZnSO_4$.

Cloning

Total RNA was extracted from *A. halleri* roots as described in Sambrook and Russell (2001). RT reactions were performed from 2 μg of total RNA using the Superscript III reverse transcriptase (Invitrogen Life Technologies) as recommended by the manufacturer (oligo dT, at 50°C). cDNAs were used immediately in PCR or kept frozen until use. Two microliters of cDNAs were used for PCR amplification. The suitability of the extracted RNAs for RT-PCR amplification was checked by performing RT-PCR control experiments with Elongation Factor 1 α (EF1α; At1g07920) using the primers EF1αF and EF1αR (Table III) in the following conditions: 94°C for 3 min followed by 35 cycles at 94°C for 30 s, 62°C for 30 s, and 72°C for 2 min using an Eppendorf Mastercycler (Eppendorf). Oligonucleotide primers (AtTcHMA4F; AtTcHMA4R: Table III) were designed to conserved regions of *HMA* cDNAs from Arabidopsis and *Thlaspi caerulescens*. The 1 kb sequence obtained was used to design the specific primer (AhHMA3′ RACE) to perform 3′ RACE amplification (following Invitrogen Life Technologies procedure). To perform the 5′ RACE amplification, the primer AhHMA5′ RACE was designed using sequences of *AhHMA4* cDNAs from Arabidopsis and *T. caerulescens*. These amplifications were cloned in pTZ57R (MBI Fermentas) and sequenced. Two specific primers AhHMA4F and AhHMA4nostpR introducing *Hin*dIII and *Bam*HI sites were designed to clone the full-length *AhHMA4* cDNA into the pYES2-GFP plasmid (Blaudez et al., 2003). The PCR conditions were the following: 95°C for 5 min followed by 24 cycles at 95°C for 30 s, 62°C for 30 s, and 68°C for 5 min using the Pfx polymerase (Invitrogen).

The direct cloning into pYES2-GFP plasmid avoided subcloning and reamplification processes leading to mutations in the sequence. A very limited number of cycles (24) was also used to limit mutations possibilities during the amplification. The insert was subsequently sequenced in both directions and checked for GFP expression in BY4741 yeast strains.

Using the AtTcHMA4F and R primers, a 1,282-bp fragment was amplified from *Alp* cDNA under the same PCR conditions as above (although 30 cycles were necessary due to the lower expression level of *HMA4*), cloned into pTZ57R, and sequenced.

Expression Analysis

The primer pair (HMA4_290F and R) used for the expression analysis was designed in a perfectly conserved coding region between *AhHM4* and *AlpHMA4* cDNAs, which were partially sequenced. The primers were tested on *AhHMA4* and *AlpHMA4* cDNAs cloned in plasmids. Both fragments (288 bp of *AhHMA4* and 291 bp of *AlpHMA4*) were amplified with equal efficiency. For RT-PCR expression analysis, total RNA was isolated from shoot and root of *A. halleri*, *A. lyrata* sp. *petraea*, the F1 individual, and the BC1 individuals with or without Cd treatment, and cDNA was obtained as described above. The amplifications were done with GoTaq Flexi DNA polymerase (Promega) using 1 μL of cDNA in a 25 μL reaction with an annealing temperature of 62°C. Two housekeeping genes were chosen to compare the relative abundance of the *HMA4* mRNAs: the EF gene *EF1α* and the ADP ribosylation factor gene *ARF* (At3g62290; Craciun et al., 2006). PCR samples were taken at successive cycles and visualized on agarose gel. The number of cycles at which a minimal signal was observed for all of the genotypes tested was chosen (24 cycles for the roots, 28 cycles for the shoots). To ensure that we were still in the linear part of the PCR amplification curve, we verified that the signal could be increased by performing more cycles. The resulting fragments were cloned into the pTZ57R plasmid (MBI Fermentas) for sequencing.

Heterologous Expression in Yeast

The truncated AhHMA4-C was amplified on the pYES2-AhHMA4-GFP plasmid using AhHMA4 specific primers designed for the C-terminal part (amino acids 720–1,161; between the end of the last transmembrane span and the stop codon) of AhHMA4. To amplify the C-terminal part, AhHMA4C/AhHMA4R or nostpR (lacking the stop codon) were used. The resulting PCR products were cloned into the *Hin*dIII-*Bam*HI-digested pYES2-GFP plasmid.

The mutation of the phosphorylation site was performed by oligonucleotide-directed PCR mutagenesis. First, a fragment was amplified by PCR with the primer pair AhHMA4F and the mutated primer AhHMA-ATPXR replacing the D401 by a G in the phosphorylation site. A second fragment was amplified with the primer pair AhHMA-ATPXF introducing the same mutations and AhHMA4R or −nostpR. DNA fragments were gel purified, mixed in a PCR mix without primers, denaturated at 95°C for 3 min, annealed at 60°C for 30 s, elongated at 68°C for 4 min, and subjected to 20 PCR cycles after the addition of AhHMA4F and AhHMA4R or −nostpR primers. The resulting *Hin*dIII-*Bam*HI fragment was cloned in pYES2-GFP plasmid. The presence of targeted mutation in all plasmid constructs was verified by DNA sequencing.

Subcellular Localization of AhHMA4 in Plant Cells

Cellular localization in plant cells was performed by transient transformation. Tobacco (*Nicotiana tabacum* 'Petit Havana') seeds were sown on soil in culture chamber and allowed to germinate and grow under long-day conditions (16-h-light/8-h-dark photoperiod) at approximately 20°C. Twenty centimeters in height tobacco plants were used for *Agrobacterium*-mediated transient expression.

To create the *35S::AhHMA4-GFP* transgene, full-length *AhHMA4* cDNA was amplified by PCR with primers AhHMA4BamF and AhHMA4KpnR (Table III) that incorporated *Bam*HI and *Kpn*I sites at the 5′ and 3′ ends of the gene, respectively. The resulting fragment was digested with *Bam*HI and *Kpn*I and cloned into corresponding sites of *pBI35S-GFP* (Tillemans et al., 2005) to yield *pBI35S::AhHMA4-GFP*. This construct as well as a control containing the *EGFP* sequence was used for transient transformation.

Transient transformation in tobacco leaves was performed essentially as described previously (Tillemans et al., 2005). Briefly, *Agrobacterium tumefaciens* bearing the appropriate binary vector was grown at 28°C overnight in 10 mL yeast extract broth liquid medium (0.5% Suc, 0.1% yeast extract, 0.5% Bactopeptone, 0.5% Invitrogen beef extract, 2 mM $MgSO_4$, pH 7.4) supplemented with 25 μg/mL gentamycin, 100 μg/mL rifampicin, and 50 μg/mL kanamycin. After centrifugation, the bacteria were washed with infiltration medium (50 mM MES, 2 mM NaH_2PO_4, 0.5% Glc, and 100 μM acetosyringone) and then resuspended in the same medium at the desired final OD_{600}. Leaves were infiltrated using a 5-mL syringe by applying gentle pressure through the stomata of the abaxial epidermis. The infiltrated areas were cut at 48 to 72 h after inoculation and further processed for confocal imaging.

Yeast Cell Staining

Yeast vacuolar membranes were selectively stained with red fluorescence probe FM4-64 (Molecular Probes, Invitrogen). This dye has been reported to stain yeast vacuolar membranes selectively (Vida and Emr, 1995). Cells (250 μL at OD_{600} 0.5) were incubated with 6 μL of FM4-64 (2 mg/mL) during 30 min at 30°C, washed twice with SD medium, and incubated 2 h before observation by confocal microscopy.

Confocal Imaging

The GFP fluorescence of yeast and plant cells was visualized by confocal laser scanning microscopy. Yeast cells and lower epidermis of agroinfiltrated leaf fragments were analyzed with an inverted Leica TCS SP2 confocal laser scanning microscope (Leica Microsystems), using a 63 × NA 1.3 Plan-Apo water-immersion objective at 1,024 × 1,024 pixel resolution. For single GFP fluorescence analyses, we used the 488 nm excitation line of an argon ion laser and the emission light was dispersed and recorded at 500 to 535 nm. For GFP and FM4-64 colocalization experiments, a second detector was activated for recording emission fluorescence at 650 to 800 nm. Images were processed with Leica software (version 2.5) and Photoshop 7.0 (Adobe Systems) software.

Protein Extraction and Gel-Blot Analysis

Yeast cells were collected by centrifugation at 5,000*g* for 1 min. Cell lysates were obtained by vortexing cells at full speed for 2 × 1 min with glass beads (420–600 μm; Sigma) in ice-cold lysis buffer containing 100 mM Tris-HCl, pH 7.5, 150 mM NaCl, 5 mM EDTA, 10% (v/v) glycerol, 100 μg/mL phenylmethylsulfonyl fluoride, 1 μg/mL leupeptin, and 10 μg/mL pepstatin A. Lysates were centrifuged at 12,000*g* for 15 min at 4°C to pellet cell debris and beads and the supernatants were centrifuged subsequently at 125,000*g* for 60 min at 4°C. Pellets (membrane fraction) were resuspended subsequently in ice-cold lysis buffer containing 10 mg/mL *n*-dodecyl-D-maltoside and incubated for 1 h on ice with occasional mixing. The extracts were centrifuged at 200,000*g* for 30 min to remove insoluble material.

Protein extracts were mixed with sample buffer (60 mM Tris-HCl, pH 6.8, 25% [v/v] glycerol, 2% [w/v] SDS, and 0.0125% [v/v] bromphenol blue) with 2-mercaptoethanol and subjected to SDS-PAGE (Laemmli, 1970) and proteins were transferred to polyvinylidene difluoride membranes (Amersham Pharmacia Biotech). Blots were probed with mouse anti-GFP antibodies (Roche; 1:1,000) and rabbit antimouse HRP-conjugated antibodies (Perbio Science; 1:10,000) were used as the secondary reagent. Proteins were revealed by enhanced chemiluminescence using the western pico revelation kit (Perbio Science) according to the manufacturer's instructions.

Determination of Intracellular Cd Content

Cells were grown for 24 h in the SD induction medium, then diluted to OD_{600} = 0.5 and grown for 48 h in 30 mL of 20 μM $CdSO_4$-containing induction medium. After centrifugation, supernatants were collected, cells were washed once with water, once with 50 mM EDTA, and then once again with water, pelleted, dried for 48 h at 60°C, and mineralized (with hydrochloric acid at 95°C). The Cd content was determined using flame atomic absorption spectroscopy (Perkin Elmer 3100 series atomic absorption spectrometer).

Accession Number and Sequence Analysis

The GenBank accession numbers for the sequence described in this article are as follows: *A. halleri* sp. *halleri*: *AhHMA4*, DQ221101; Arabidopsis: *AtHMA4*, NM127468; *T. caerulescens*: *TcHMA4*, AJ567384; *A. lyrata* sp. *petraea*: *AlpHMA4*, EF176604. Alignment of HMA4 sequences was performed using ClustalW (Thompson et al., 1994) and was manually adjusted.

ACKNOWLEDGMENTS

We thank Ute Krämer (Max Planck Institut, Golm, Germany) for the gift of the *zrc1/cot1* mutant yeast strain and Damien Blaudez (Université Henri Poincare, Nancy, France) for providing the pYES2-GFP plasmid. We acknowledge J.A.C. Smith (Oxford University, Oxford) for proofreading and discussion and Piétro Salis and Geoffrey Gosset (Université Libre de Bruxelles, Brussels) for practical help.

Received December 20, 2006; accepted April 5, 2007; published April 13, 2007.

LITERATURE CITED

Axelsen KB, Palmgren MG (2001) Inventory of the superfamily of P-type ion pumps in Arabidopsis Plant Physiol **126:** 696–706

Baxter I, Tchieu J, Sussman MR, Boutry M, Palmgren MG, Gribskov M, Harper JF, Axelsen KB (2003) Genomic comparison of P-type ATPase ion pumps in Arabidopsis and rice. Plant Physiol **132:** 618–628

Beavis WD, Smith OS, Grant D, Fincher R (1994) Identification of quantitative trait loci using a small sample of topcrossed and F4 progeny from maize. Crop Sci **34:** 882–896

Becher M, Talke IN, Krall L, Kramer U (2004) Cross-species microarray transcript profiling reveals high constitutive expression of metal homeostasis genes in shoots of the zinc hyperaccumulator *Arabidopsis halleri*. Plant J **37:** 251–268

Bernard C, Roosens N, Czernic P, Lebrun M, Verbruggen N (2004) A novel CPx-ATPase from the cadmium hyperaccumulator *Thlaspi caerulescens*. FEBS Lett **569:** 140–148

Bert V, Bonnin I, Saumitou-Laprade P, de Laguerie P, Petit D (2002) Do *Arabidopsis halleri* from nonmetallicolous populations accumulate zinc and cadmium more effectively than those from metallicolous populations? New Phytol **155:** 47–57

Bert V, Meerts P, Saumitou-Laprade P, Salis P, Gruber W, Verbruggen N (2003) Genetic basis of Cd tolerance and hyperaccumulation in *Arabidopsis halleri*. Plant Soil **249:** 9–18

Blaudez D, Kohler A, Martin F, Sanders D, Chalot M (2003) Poplar metal tolerance protein 1 confers zinc tolerance and is an oligomeric vacuolar zinc transporter with an essential leucine zipper motif. Plant Cell **15:** 2911–2928

Bradshaw HD, Otto KG, Frewen BE, McKay JK, Schemske DW (1998) Quantitative trait loci affecting differences in floral morphology between two species of monkeyflower (*Mimulus*). Genetics **149:** 367–382

Clemens S (2006) Toxic metal accumulation, responses to exposure and mechanisms of tolerance in plants. Biochimie **88:** 1707–1719

Clemens S, Bloss T, Vess C, Neumann D, Nies DH, zur Nieden U (2002) A transporter in the endoplasmic reticulum of *Schizosaccharomyces pombe* cells mediates zinc storage and differentially affects transition metal tolerance. J Biol Chem **277:** 18215–18221

Craciun AR, Courbot M, Bourgis F, Salis P, Saumitou-Laprade P, Verbruggen N (2006) Comparative cDNA-AFLP analysis of Cd-tolerant and -sensitive genotypes derived from crosses between the Cd hyperaccumulator *Arabidopsis halleri* and *Arabidopsis lyrata* ssp. *petraea*. J Exp Bot **57:** 2967–2983

Deniau A, Pieper B, Ten Bookum WM, Lindhout P, Aarts MGM, Schat H (2006) QTL analysis of cadmium and zinc accumulation in the heavy metal hyperaccumulator *Thlaspi caerulescens*. Theor Appl Genet **113:** 907–920

Dräger DB, Desbrosses-Fonrouge AG, Krach C, Chardonnens AN, Meyer RC, Saumitou-Laprade P, Kramer U (2004) Two genes encoding *Arabidopsis halleri* MTP1 metal transport proteins co-segregate with zinc tolerance and account for high MTP1 transcript levels. Plant J **39:** 425–439

Eren E, Arguello JM (2004) Arabidopsis HMA2, a divalent heavy metal-transporting P-IB-type ATPase, is involved in cytoplasmic Zn2+ homeostasis. Plant Physiol **136:** 3712–3723

Filatov V, Dowdle J, Smirnoff N, Ford-Lloyd B, Newbury HJ, Macnair MM (2006) Comparison of gene expression in segregating families identifies genes and genomic regions involved in a novel adaptation, zinc hyperaccumulation. Mol Ecol **15:** 3045–3059

Gietz RD, Woods RA (2002) Transformation of yeast by lithium acetate/single-stranded carrier DNA/polyethylene glycol method. Methods Enzymol **350:** 87–96

Hussain D, Haydon MJ, Wang Y, Wong E, Sherson SM, Young J, Camakaris J, Harper JF, Cobbett CS (2004) P-type ATPase heavy metal transporters with roles in essential zinc homeostasis in Arabidopsis Plant Cell **16:** 1327–1339

Krämer U (2005) Phytoremediation: novel approaches to cleaning up polluted soils. Curr Opin Biotechnol **16:** 133–141

Kuittinen H, de Haan AA, Vogl C, Oikarinen S, Leppälä J, Koch M, Mitchell-Olds T, Langley CH, Savolainen O (2004) Comparing the linkage maps of the close relatives *Arabidopsis lyrata* and *A. thaliana*. Genetics **168:** 1575–1584

Laemmli UK (1970) Cleavage of structural proteins during assembly of head of bacteriophage-T4. Nature **227:** 680–681

Macnair MR (1987) Heavy metal tolerance in plants: a model evolutionary system. Trends Ecol Evol **2:** 354–359

Macnair MR, Bert V, Huitson SB, Saumitou-Laprade P, Petit D (1999) Zinc tolerance and hyperaccumulation are genetically independent characters. Proc Biol Sci **266:** 2175–2179

Mills RF, Francini A, da Rocha PSCF, Baccarini PJ, Aylett M, Krijger GC, Williams LE (2005) The plant P-1B-type ATPase AtHMA4 transports Zn and Cd and plays a role in detoxification of transition metals supplied at elevated levels. FEBS Lett **579:** 783–791

Mills RF, Krijger GC, Baccarini PJ, Hall JL, Williams LE (2003) Functional expression of AtHMA4, a P-1B-type ATPase of the Zn/Co/Cd/Pb subclass. Plant J **35:** 164–176

Oetting WS, Lee HK, Flanders DJ, Wiesner GL, Sellers TA, King RA (1995) Linkage analysis with multiplexed short tandem repeat polymorphism using infrared fluorescence and M13 tailed primers. Genomics **30:** 450–458

Orr HA (1998) Testing natural selection vs. genetic drift in phenotypic evolution using quantitative trait locus data. Genetics **149:** 2099–2104

Papoyan A, Kochian LV (2004) Identification of *Thlaspi caerulescens* genes that may be involved in heavy metal hyperaccumulation and tolerance: characterization of a novel heavy metal transporting ATPase. Plant Physiol **136:** 3814–3823

Pauwels M, Frérot H, Bonnin I, Saumitou-Laprade P (2006) A broad-scale analysis of population differentiation for Zn tolerance in an emerging model species for tolerance study: *Arabidopsis halleri* (Brassicaceae). J Evol Biol **19:** 1838–1850

Pence NS, Larsen PB, Ebbs SD, Letham DL, Lasat MM, Garvin DF, Eide D, Kochian LV (2000) The molecular physiology of heavy metal transport in the Zn/Cd hyperaccumulator *Thlaspi caerulescens*. Proc Natl Acad Sci USA **97:** 4956–4960

Pollard AJ, Powell KD, Harper FA, Smith JAC (2002) The genetic basis of metal hyperaccumulation in plants. CRC Crit Rev Plant Sci **21:** 539–566

Rensing C, Ghosh M, Rosen BP (1999) Families of soft-metal-ion-transporting ATPases. J Bacteriol **181:** 5891–5897

Sambrook J, Russell D (2001) Molecular Cloning: A Laboratory Manual, Ed 3. Cold Spring Harbor Laboratory Press, Cold Spring Harbor, NY

SAS (1999) SAS OnLineDoc V8. Statistical Analysis System Institute, Cary, NC

Schat H, Ten Bookum WM (1992) Genetic control of copper tolerance in Silene vulgaris. Heredity **70:** 142–147

Talke I, Hanikenne M, Krämer U (2006) Zinc dependent global transcriptional control, transcriptional de-regulation and higher gene copy number for genes in metal homeostasis of the hyperaccumulator *Arabidopsis halleri*. Plant Physiol **142:** 148–167

Thompson JD, Higgins DG, Gibson TJ (1994) Clustal-W—improving the sensitivity of progressive multiple sequence alignment through sequence weighting, position-specific gap penalties and weight matrix choice. Nucleic Acids Res **22:** 4673–4680

Tillemans V, Dispa L, Remacle C, Collinge M, Motte P (2005) Functional distribution and dynamics of *Arabidopsis* SR splicing factors in living plant cells. Plant J **41:** 567–582

van de Mortel J, Villanueva LA, Schat H, Kwekkeboom J, Coughlan S, Moerland PD, Ver Loren van Themaat E, Koornneef M, Aarts MGM (2006) Large expression differences in genes for iron and zinc homeostasis, stress response, and lignin biosynthesis distinguish roots of *Arabidopsis thaliana* and the related metal hyperaccumulator *Thlaspi caerulescens*. Plant Physiol **142:** 1127–1147

Van Ooijen JW, Boer MP, Jansen RC, Maliepaard C (2002) MapQTL 4.0, Software for the Calculation of QTL Positions on Genetic Maps. Plant Research International, Wageningen, The Netherlands

Van Ooijen JW, Voorips RE (2001) Joinmap 3.0, Software for the Calculation of Genetic Linkage Maps. Plant Research International, Wageningen, The Netherlands

Van Rossum F, Bonnin I, Fenart S, Pauwels M, Petit D, Saumitou-Laprade P (2004) Spatial genetic structure within a metallicolous population of *Arabidopsis halleri*, a clonal, self-incompatible and heavy-metal-tolerant species. Mol Ecol **13:** 2959–2967

Verret F, Gravot A, Auroy P, Leonhardt N, David P, Nussaume L, Vavasseur A, Richaud P (2004) Overexpression of AtHMA4 enhances root-to-shoot translocation of zinc and cadmium and plant metal tolerance. FEBS Lett **576:** 306–312

Verret F, Gravot A, Auroy P, Preveral S, Forestier C, Vavasseur A, Richaud P (2005) Heavy metal transport by AtHMA4 involves the N-terminal degenerated metal binding domain and the C-terminal His(11) stretch. FEBS Lett **579:** 1515–1522

Vida TA, Emr SD (1995) A new vital stain for visualizing vacuolar membrane dynamics and endocytosis in yeast. J Cell Biol **128:** 779–792

Voorrips RE (2002) MapChart: software for the graphical presentation of linkage maps and QTLs. J Hered **93:** 77–78

Weber M, Harada E, Vess C, von Roepenack-Lahaye E, Clemens S (2004) Comparative microarray analysis of *Arabidopsis thaliana* and *Arabidopsis halleri* roots identifies nicotianamine synthase, a ZIP transporter and other genes as potential metal hyperaccumulation factors. Plant J **37:** 269–281

Willems G, Dräger DB, Courbot M, Godé C, Verbruggen N, Saumitou-Laprade P (2007) Quantitative trait loci mapping of zinc tolerance in the metallophyte *Arabidopsis halleri* ssp. *halleri*. Genetics doi/10.1534/genetics.106.064485